JOURNAL OF SPACECRAFT AND ROCKETS
Vol. 46, No. 1, January–February 2009

Method for Prediction and Optimization of a Stratospheric Balloon Ascent Trajectory

Gianfranco Morani,* Roberto Palumbo,† Giovanni Cuciniello,‡ Federico Corraro,§ and Michelangelo Russo¶
Italian Aerospace Research Center, 81043 Capua, Italy

DOI: 10.2514/1.39469

In this paper, we propose a methodology for the prediction and optimization of the ascent trajectory of a stratospheric balloon to target a specified three-dimensional area. The methodology relies mainly on the Analysis Code for High-Altitude Balloons, a simulation tool for the prediction of flight trajectory and thermal behavior of high-altitude, zero-pressure balloons, and on a statistical analysis for estimating the trajectory prediction errors. The paper also describes the algorithms used for balloon parameter optimization to obtain a flight trajectory that reaches a predefined target area without any ballast drop or gas venting control. The proposed methodology was successfully used during the first Dropped Transonic Flight Test of the Flying Test Bed 1 demonstrator accomplished on 24 February 2007 by the Italian Aerospace Research Center. The reported postflight analysis of all the test campaign demonstrates that the proposed methodology for trajectory prediction and optimization guarantees very satisfactory and reliable results for both the selection of the best day to perform such a mission and the definition of the correct balloon parameters to be used for targeting a predefined three-dimensional area.

Nomenclature

A_D = reference area for drag force computation, m^2
$A(h)$ = event identifying the interception of the release zone at altitude h
C_D = drag force coefficient
$E[\zeta]$ = expected value of the random variable ζ
$e_{v_{\text{east}}}$ = prediction error of east velocity component, m/s
$e_{v_{\text{north}}}$ = prediction error of north velocity component, m/s
F_L = free lift
f = equivalent form of free lift
f_x = probability density function of the random variables x
$f_{x,y}$ = joint probability density function of the random variables x, y
$f_{y|x}$ = probability density function of the random variable y conditioned to the variable x
$f_{\max}$ = maximum structural free lift
$f_{\min}$ = minimum structural free lift
$\bar{f}_{\max}$ = maximum free lift guaranteeing a success probability p_0
$\bar{f}_{\min}$ = minimum free lift guaranteeing a success probability p_0
f_{opt} = optimum free lift
g = gravity acceleration, m/s^2
h = altitude, m
I_1 = prediction reliability index
I_2 = missed launch index
k = scaling factor between different rate of climb profiles
$L_{\bar{\tau}}$ = average fractional free lift
$\hat{L}_{\bar{\tau}}$ = reference average fractional free lift
M_{gas} = mass of gas, kg
M_{gr} = total load mass, kg
M_{bal} = ballast loaded onboard, kg
$M_{\text{opt}}^{\text{gas}}$ = optimum mass of gas, kg
$P_{\text{east}}(h)$ = probability of intercepting the release zone in terms of longitude at altitude h
$P_{\text{good}}(h)$ = probability of intercepting the release zone at altitude h
$P_{\text{north}}(h)$ = probability of intercepting the release zone in terms of latitude at altitude h
$\bar{P}_{\text{good}}$ = probability of having a successful trajectory
$\hat{P}_{\text{good}}$ = estimation of probability of having a successful trajectory
P_{opt} = optimum success probability
$\Pr\{\Omega\}$ = probability of the event Ω
p_0 = minimum allowable success probability
R_e = projection of Earth's radius on local parallel, m
R_n = Earth's radius, m
S_x, S_y = events identifying the success of the predicted and actual trajectory, respectively
t_h = instant at which the predicted ascent trajectory reaches altitude h, s
$t_{h_{\text{act}}}$ = instant at which the actual ascent trajectory reaches altitude h, s
V_z = rate of climb of the predicted trajectory, m/s
$\hat{V}_z$ = reference rate of climb of the predicted trajectory, m/s
x = generic variable identifying the predicted trajectory
y = generic variable identifying the actual trajectory
$\Delta\vartheta$ = longitude prediction error, rad

Received 1 July 2008; revision received 29 October 2008; accepted for publication 8 November 2008.

*Researcher, Flight Systems Department; g.morani@cira.it.
†Researcher, Flight Systems Department; r.palumbo@cira.it. Member AIAA.
‡Researcher, Flight Systems Department; g.cuciniello@cira.it.
§Senior Researcher, Flight Systems Department; f.corraro@cira.it.
¶Researcher, Flight Systems Department; mi.russo@cira.it. Member AIAA.

$\Delta\lambda$ = latitude prediction error, rad
$\Delta\vartheta_{\min}(h)$, $\Delta\vartheta_{\max}(h)$ = minimum and maximum allowable longitude prediction error at altitude h, rad
$\Delta\lambda_{\min}(h)$, $\Delta\lambda_{\max}(h)$ = minimum and maximum allowable latitude prediction error at altitude h, rad
$\Delta V^{\text{east}}_{\min}(h)$, $\Delta V^{\text{east}}_{\max}(h)$ = minimum and maximum allowable east velocity prediction error at altitude h, m/s
$\Delta V^{\text{north}}_{\min}(h)$, $\Delta V^{\text{north}}_{\max}(h)$ = minimum and maximum allowable north velocity prediction error at altitude h, m/s
$\Delta M_g^{\text{lower}}$, $\Delta M_g^{\text{upper}}$ = minimum and maximum allowable uncertainty on gas mass, kg
ϑ = longitude, deg
$\vartheta_{\min}$, $\vartheta_{\max}$ = lower and upper longitude of the rectangular safe release zone, deg
λ = latitude, deg
$\lambda_{\min}$, $\lambda_{\max}$ = lower and upper latitude of the rectangular safe release zone, deg
ρ_{air} = atmospheric density, kg/m^3
σ = ratio between the molecular weight of the air and the molecular weight of the gas
$\sigma_{ev_{\text{east}}}$ = standard deviation of prediction error of east velocity component, m/s
$\sigma_{ev_{\text{nor}}}$ = standard deviation of prediction error of north velocity component, m/s
$\sigma_{\Delta\vartheta}$ = standard deviation of longitude prediction error, rad
$\sigma_{\Delta\lambda}$ = standard deviation of latitude prediction error, rad
τ = ratio between the air temperature and the gas temperature
$\bar{\tau}$ = average value of τ during ascent

Subscripts

1 = relative to the predicted trajectory
2 = relative to the actual trajectory

Superscript

() = time derivative

I. Introduction

THE scientific community often relies on high-altitude, zero-pressure balloons to carry out different kinds of experiments in a near-space environment. To comply with the objectives of a balloon mission, it is usually necessary to predict, monitor, and track the flight trajectory. Balloon trajectory prediction, however, is a challenging problem [1–7]. Indeed, after liftoff, a balloon can be considered a thermal and dynamic system that is practically in free evolution inside a complex thermal environment and subject to atmospheric winds. Consequently, balloon mission preparation requires an accurate and reliable prediction methodology to plan the mission successfully while satisfying possible safety constraints imposed by the flight.

In the framework of the aerospace research national program, the Italian Aerospace Research Center (CIRA) is conducting a program named USV (Unmanned Space Vehicles). The objective of the USV project [8] is to design and manufacture two unmanned flying test bed (FTB) vehicles (FTB1 for atmospheric flights and FTBX for sustained hypersonic demonstrations), conceived as flying laboratories to test advanced functionalities and critical operational aspects peculiar to the future reusable launch vehicle. The nominal atmospheric mission profile, named Dropped Transonic Flight Test (DTFT), is based on a drop of the FTB1 vehicle from a stratospheric balloon at an altitude between 19 and 21 km inside a specific target area (safe release zone), lifting off from a launch base located in Arbatax, Sardinia, Italy (see Fig. 1). This mission profile requires an accurate ascent trajectory prediction and preflight optimization of the key parameters of the balloon system to maximize the success probability of the mission while guaranteeing all the safety constraints.

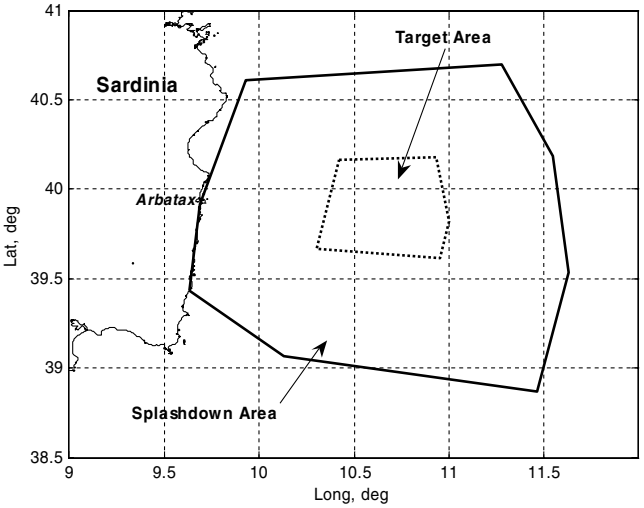

Fig. 1 Target area/safe splashdown area.

To fulfill these stringent requirements, CIRA has developed the Analysis Code for High-Altitude Balloons (ACHAB) [1], a specific simulation software able to predict 3-D flight trajectory and thermal behavior of high-altitude, zero-pressure balloons and a set of important prediction and optimization methodologies that are the main subject of this paper.

In the last years, some efforts have been made to develop flight prediction and trajectory optimization for stratospheric balloons ([9–14] and references therein). In these papers, balloon trajectory prediction is performed, taking into account several trajectory prediction sources of uncertainty (wind velocity, gas mass, air temperature, etc.). In particular, wind uncertainty is computed using forecast models as well as soundings. This is accomplished through a statistical analysis on the (latitudinal) distance between the predicted and actual trajectories. The analysis results are then used to compute the levels of probability related to the interception of a target area for each predicted trajectory. The obtained results, however, could be heavily dependent on the altitude profile chosen for the analysis, being the distance between the trajectories strongly related to the time to reach the target point. For what concerns trajectory optimization, prediction capabilities are exploited to compute an optimal sequence of maneuvers aimed at achieving the desired mission goals. However, the overall uncertainties are not explicitly taken into account during the preflight optimization process. Therefore, this kind of optimization may lead to a nonoptimal mission trajectory because of the actual wind profiles encountered during flight that could be quite different from the expected ones.

In this paper, we propose a different method for prediction and optimization of the ascent trajectory of stratospheric balloons. The proposed method directly takes into account the uncertainties related to the balloon parameters (mainly gas mass) and wind forecast to obtain a solution that maximizes the probability to reach a target area without any ballast drop or gas venting control. Based on this method, an operative procedure has been defined (supporting the decision-making process during the prelaunch phase) and a navigation software tool was developed [15] (supporting the balloon flight operations and possible ballast jettison) to accomplish the mission. The proposed method has been successfully used during the first DTFT1 mission carried out on 24 February 2007 from Arbatax (Sardinia), Italy.

The paper is organized as follows. The method for prediction and optimization of balloon trajectory is described in Secs. II and III. The description of the operative procedure is described in Sec. IV,

whereas a postflight analysis of DTFT1 test campaign is discussed in Sec. V. Finally, Sec. VI contains some brief concluding remarks.

II. Prediction of Ascent Trajectory

A. Preliminary Analysis of Sounding and Forecast Prediction Capability

In this section, a preliminary analysis is performed to decide whether sounding data or European Center for Medium-Range Weather Forecasts (ECMWF) wind forecast data are more suitable to accomplish an accurate balloon trajectory prediction. In fact, several approaches to trajectory prediction [9–14] heavily rely on the soundings carried out some hours before the launch, considering these data more reliable than the forecast ones. Our analysis, however, will show that forecast data are more reliable.

To perform this analysis, two reliability indices have been defined for trajectory prediction:

1) The Prediction Reliability Index I_1 is the probability of having a successful (i.e., satisfying a given criterion) trajectory when the predicted trajectory is successful itself.

2) The "Missed Launch" Index I_2 is the probability of making a wrong prediction, that is, predicting a trajectory as unsuccessful when the actual trajectory is successful.

This analysis has been accomplished exploiting three trajectory databases (soundings, forecast, and actual trajectories) built using ACHAB and the ECMWF atmospheric and wind data relative to Arbatax (DTFT1 mission launch base) during the years 2004–2006. More in detail, "sounding" trajectories have been obtained using ECMWF historical analysis data, at the hours of the sounding (6 h before the launch) whereas forecast trajectories have been obtained using ECMWF wind forecasts (available 18 h before the launch). Finally, the "actual" trajectories have been obtained using ECMWF historical analysis data at 06 UTC (Coordinated Universal Time) (note that, although true launch hour was 07 UTC, the ECMWF data were available only for 06 UTC).

For what concerns the computation of the preciously defined indices, two different kinds of predictions have been used: a sounding-based trajectory prediction (using the sounding database) and a forecast-based prediction (using forecast database). In any case, the predicted trajectories have been tagged as successful if they satisfied given safety and mission requirements. The results of the comparative analysis are shown in Table 1. Given that more than 170 simulated trajectories were used for this analysis, it is possible to show (see [16]) that the results of Table 1 have a maximum error (accuracy) of 10%, with a probability greater than 90%. These results show the poor reliability of the sounding-based predictions with respect to the forecast-based ones. This fact is not surprising because, although sounding data guarantee better accuracy on wind status than the forecast data, they refer to an atmospheric condition which may be significantly different from the one at the actual hour of flight.

B. Statistical Characterization of Trajectory Prediction Error

Once chosen which set of wind data was more suitable for accurate trajectory prediction, we carried out a statistical characterization of the prediction error in terms of "distance" between the predicted and the actual trajectories, for each ECMWF forecast at −6, −18, −30, −42, −54, and −66 h before the launch.

To define the trajectory prediction error, an important assumption has to be made, that is, the horizontal velocity of the balloon is considered to be always equal to the horizontal velocity of the wind. Strictly speaking, this assumption implies instant adjustment of the balloon's horizontal velocity as it moves from one air stratum to another where the wind velocity is different (see [2]). It should be noted that such behavior does not reflect what actually happens during some of the flight phases (liftoff, tropopause transition, stratospheric oscillations, or local wind shears). Nevertheless, it can be globally considered true because the average acceleration over long portions of the flight is always practically zero.

Table 1 Prediction reliability of sounding and forecast data

	Prediction reliability index I_1	Missed launch index I_2
Sounding data	75.3%	13.6%
Forecast data	95%	11.8%

In what follows, we will consider only the effects of the prediction errors on the wind profile, neglecting the uncertainty on the vertical velocity component of the balloon which is mainly related to atmospheric forecast data (air temperature and pressure), gas mass, and thermodynamic model. Although we neglect this uncertainty in the characterization of prediction error, however, we account for gas mass errors in the optimization procedure (see Sec. III). Moreover, for what concerns air temperature and pressure, in this work we will consider their errors negligible with respect to gas mass errors. Anyway, their influence on the vertical velocity is currently under investigation and will be part of future work. Finally, the errors due to the balloon thermodynamic model are discussed in [1] and will not be considered in this paper. However, their effect can be regarded as less influential than the ones related to the other sources of uncertainty considered hereafter (see [14]).

The characterization of the trajectory prediction error is related to the error on the wind velocity components (north and east). In other words, the following variables have been considered:

$$e_{v_{\text{east}}}(h) \stackrel{\text{def}}{=} R_e \frac{\Delta\vartheta(h)}{t_h} \qquad e_{v_{\text{north}}}(h) \stackrel{\text{def}}{=} R_n \frac{\Delta\lambda(h)}{t_h} \tag{1}$$

where h is the altitude, $\Delta\vartheta$ and $\Delta\lambda$ are the longitude and latitude prediction errors (in radians), respectively, t_h is the instant at which the predicted trajectory reaches the altitude h, and R_n and R_e are the Earth's radius and its projection on the local parallel, respectively. Using the preceding definitions, it is possible to evaluate (for each altitude) the difference in velocity necessary to null out the longitude (latitude) error under the hypothesis that velocity is constant from t_0 to t_h and that these errors do not depend on latitude and longitude. This last assumption can be justified considering that, above a certain altitude, the wind prediction error is mainly due to the wind model inaccuracy and not to the specific geography of the launch site. Furthermore, the "velocity errors" have been assumed to have Gaussian statistical distribution. This assumption has been confirmed by the numeric calculation of the cumulative distribution function for the variables of interest. The characterization of Eq. (1) is quite general and can be considered almost independent of the actual balloon rate of climb. In fact, let us consider the error related to the east component of the wind velocity (the same conclusions hold for the north component). Letting $V(t) \stackrel{\text{def}}{=} R_e \dot{\vartheta}(t)(\pi/180)$, we can write the velocity error as

$$\begin{aligned} e_{v_{\text{east}}}(h) &= \frac{R_e}{t_h}[\vartheta_2(h) - \vartheta_1(h)]\frac{\pi}{180} \\ &= \frac{1}{t_h}\left[\int_0^{t_{h_{\text{act}}}} V_2(t)\,\mathrm{d}t - \int_0^{t_h} V_1(t)\,\mathrm{d}t\right] \cong \frac{1}{t_h}\int_0^{t_h}[V_2(t) - V_1(t)]\,\mathrm{d}t \end{aligned} \tag{2}$$

where the subscript 2 refers to the actual trajectory, and the subscript 1 refers to the forecast made a number of hours before. In Eq. (2), we assumed that $t_{h_{\text{act}}} \cong t_h$, based on the explanation at the beginning of this section about error sources other than wind profiles. Performing a change of variables (from the variable "time" to the variable "altitude") we have

$$e_{v_{\text{east}}}(h) \cong \frac{1}{t_h}\int_0^h \frac{[V_2(z) - V_1(z)]}{V_z(z)}\,\mathrm{d}z \tag{3}$$

where $V_z(t) = \mathrm{d}z/\mathrm{d}t$ is the predicted rate of climb of the stratospheric balloon. By rewriting the instant t_h as the integral in the variable altitude z,

$$t_h = \int_0^{t_h} \mathrm{d}t = \int_0^h \frac{1}{V_z(z)}\,\mathrm{d}z \tag{4}$$

the variable $e_{v_{\text{east}}}(h)$ can be written as

$$e_{v_{\text{east}}}(h) \cong \frac{\int_0^h \{[(V_2(z) - V_1(z)]/V_z(z)\}\,\mathrm{d}z}{\int_0^h [1/V_z(z)]\,\mathrm{d}z} \tag{5}$$

Now, if the rate of climb can be written as a scaled version of a reference profile $\hat{V}_z$, that is,

$$V_z(z) = k\hat{V}_z(z) \tag{6}$$

we have

$$e_{v_{\text{east}}}(h) \cong \frac{\int_0^h \{[(V_2(z) - V_1(z)]/\hat{V}_z(z)\}\,\mathrm{d}z}{\int_0^h [1/\hat{V}_z(z)]\,\mathrm{d}z} \tag{7}$$

for any constant k and thus for every rate of climb profile. The hypothesis that allows us to write the rate of climb as a scaled version of a reference profile can be justified through the following considerations. Let us start from the vertical equation of motion of a balloon under zero vertical acceleration [2]:

$$(\text{Drag})_z = -(M_{\text{gr}} + M_{\text{bal}})g\left[1 + \mu\left(1 - \frac{\sigma}{\tau}\right)\right] \tag{8}$$

where $\mu = M_{\text{gas}}/(M_{\text{gr}} + M_{\text{bal}})$, M_{gas} is the mass of gas, M_{gr} is the total load mass (balloon film, payload, flight chain, etc.) without ballast and gas, M_{bal} is the ballast loaded onboard, σ is the ratio between the molecular weight of the air and the molecular weight of the gas, and τ is the ratio between the air temperature and the gas temperature. Under the hypothesis that the horizontal velocity of the balloon can be considered always equal to the horizontal velocity of the wind and, moreover, that $\tau \cong \bar{\tau} = \text{const}$ during the ascent trajectory, we can write the vertical velocity as

$$V_z = \sqrt{\frac{2(M_{\text{gr}} + M_{\text{bal}})gL_{\bar{\tau}}}{\rho_{\text{air}} C_D A_D}} \tag{9}$$

where $L_{\bar{\tau}} = \mu[(\sigma/\bar{\tau}) - 1] - 1$ is an *average fractional free lift* and it is representative of the average free lift along the trajectory. If the preceding hypotheses are valid, all the quantities in Eq. (9) except for $L_{\bar{\tau}}$ can be considered as a function of the altitude only. Then, we have the following relationship between V_z and $L_{\bar{\tau}}$:

$$V_z(h, F_L) = a(h)\sqrt{L_{\bar{\tau}}} \tag{10}$$

with $a(h)$ being a function of the altitude. Therefore, if we consider a reference average free lift $\hat{L}_{\bar{\tau}}$ and the related vertical velocity $\hat{V}_z(h, \hat{L}_{\bar{\tau}}) = a(h)\sqrt{\hat{L}_{\bar{\tau}}}$, all the vertical velocity profiles will be obtained by simply scaling $\hat{V}_z$, that is,

$$V_z(h, L_{\bar{\tau}}) = k\hat{V}_z(h, \hat{L}_{\bar{\tau}}) \tag{11}$$

where $L_{\bar{\tau}} = k^2\hat{L}_{\bar{\tau}}$. It is worth remarking that, although the function $a(h)$ depends on the daily local atmospheric conditions, we can consider air temperature and pressure similar to those of the standard midlatitude winter atmospheric model and therefore time invariant. In view of these considerations, the analysis carried out is always valid provided that local and seasonal atmospheric conditions are not much different from the aforementioned atmospheric model. Figure 2 shows the standard deviation of the east velocity prediction error (as a function of altitude) between the actual trajectory and the trajectory predicted 18 h before.

Starting from the preceding statistical characterization of the velocity error, it is possible to obtain directly (for each altitude) dispersion areas having the shape of an ellipse in the longitude–latitude plane. These ellipses are centered on the predicted trajectory and give indication about the true position of the balloon trajectory with a confidence of 99.7% (3σ for a Gaussian variable). This approach is particularly attractive, as it does not require any Monte Carlo analysis to obtain the trajectory dispersion areas due to wind forecast uncertainties, thus allowing a very quick computation of such areas and making them suitable for an optimization

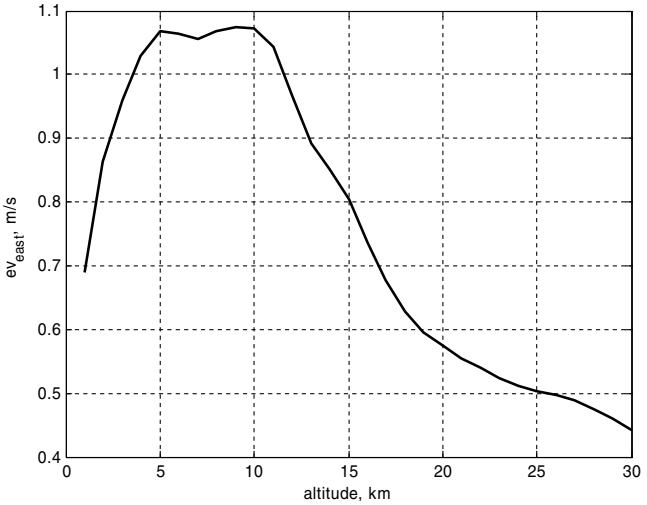

Fig. 2 East velocity error as a function of altitude (forecast).

algorithm. The dispersion ellipses are drawn starting from the velocity errors previously defined. Let $\sigma_{ev_{\text{east}}}$ and $\sigma_{ev_{\text{nor}}}$ be the standard deviations of these errors. The standard deviations of position errors $\Delta\vartheta$, $\Delta\lambda$ can be written as [see Eq. (1)]

$$\begin{aligned} \Delta\vartheta(h) &= \frac{e_{v_{\text{east}}}(h)t_h}{R_e} \Rightarrow \sigma_{\Delta\vartheta}(h) = \frac{\sigma_{ev_{\text{east}}}(h)t_h}{R_e} \\ \Delta\lambda(h) &= \frac{e_{v_{\text{north}}}(h)t_h}{R_n} \Rightarrow \sigma_{\Delta\lambda}(h) = \frac{\sigma_{ev_{\text{nor}}}(h)t_h}{R_n} \end{aligned} \tag{12}$$

These two standard deviations are used to draw an ellipse having as semi-axes $3.4393\sigma_{\Delta\vartheta}(h)$ and $3.4393\sigma_{\Delta\lambda}(h)$. In fact, if we consider the velocity errors as two Gaussian and independent random variables, the same conclusion will hold for the position errors obtained through Eqs. (12) (see [17]). In this case, the probability that the position errors are limited within an area having the shape of an ellipse will depend only on the ellipse's radii (see [17]), and so it is possible to find the length of each radius (with respect to the standard deviation) that guarantees a probability of 99.7%. It is worth remarking that these ellipses are dependent on the trajectory rate of climb. In fact, although we can consider $\sigma_{ev_{\text{east}}}$ and $\sigma_{ev_{\text{nor}}}$ almost independent of the rate of climb, the time instant t_h is strongly dependent on it [see Eq. (4)]. Therefore, the slower the ascent trajectories are, the larger the horizontal dispersions will be, and vice versa. The physical meaning of this assertion is straightforward because the velocity error implies a displacement (from the predicted horizontal trajectory) which monotonically increases with time. The dispersion areas computed in such a way have been employed for both offline and online [15] prediction and optimization methods.

III. Balloon Trajectory Optimization

The uncertainty of the wind forecast makes it difficult to choose the proper amount of gas mass necessary to obtain, with a reasonable safety margin, the desired trajectory that reaches the final target area. In addition, inflation procedures at launch do not allow the exact knowledge of the actual mass of gas transferred to the balloon. These two main concerns make the ascent trajectory optimization a challenging problem.

The parameter that usually identifies the balloon ascent force, at least right after liftoff when the aerodynamic forces are negligible and the ratio between the temperature of air and gas is close to 1, is the starting fractional free lift (or simply free lift hereinafter) $F_L = \mu(\sigma - 1) - 1$ (see [2]). For the sake of simplicity, we will use the following equivalent form:

$$f = 1 + F_L = \mu(\sigma - 1) \tag{13}$$

In this section, we will describe a trajectory optimization algorithm that allows the determination of the optimal free lift, with

respect to mission objectives (i.e., reaching the target area), while taking into account wind uncertainties without any ballast drop or gas venting control.

The optimization problem has been solved with a probabilistic approach: the optimal free lift will be the one maximizing the probability that the ascent trajectory intercepts the release zone depicted in Fig. 1. This probability can be computed, for each free lift, starting from the statistical characterization of the trajectory prediction error (see Sec. II). More in detail, let

$$\Delta\vartheta_{\min}(h) = [\vartheta_{\min} - \vartheta(h)]\frac{\pi}{180} \qquad \Delta\vartheta_{\max}(h) = [\vartheta_{\max} - \vartheta(h)]\frac{\pi}{180}$$
$$\Delta\lambda_{\min}(h) = [\lambda_{\min} - \lambda(h)]\frac{\pi}{180} \qquad \Delta\lambda_{\max}(h) = [\lambda_{\max} - \lambda(h)]\frac{\pi}{180} \tag{14}$$

be the trajectory errors as a function of the altitude h with respect to $\vartheta_{\min}, \vartheta_{\max}, \lambda_{\min}, \lambda_{\max}$ which define a rectangular safe release zone in terms of longitude and latitude. It is worth noting that, even if the actual safe release zone is not rectangular (see Fig. 1), it is always possible to approximate it by the union of a finite number of nonoverlapping rectangles and thus compute the interception probability by simply summing the probabilities computed over each rectangular zone (the interception of each rectangular zone is an exclusive event).

Now, we can convert the errors in Eqs. (14) into velocity errors by appropriate scaling [see Eq. (1)], thus obtaining $\Delta V^{\text{east}}_{\min}(h)$, $\Delta V^{\text{east}}_{\max}(h)$, $\Delta V^{\text{north}}_{\min}(h)$, and $\Delta V^{\text{north}}_{\max}(h)$. Therefore, the probability of having a trajectory error not greater than the maximum allowable one can be expressed as

$$\begin{aligned} P_{\text{east}}(h) &= \Pr\{\Delta V^{\text{east}}_{\min}(h) \le \Delta V_{\text{east}}(h) \le \Delta V^{\text{east}}_{\max}(h)\} \\ P_{\text{north}}(h) &= \Pr\{\Delta V^{\text{north}}_{\min}(h) \le \Delta V_{\text{north}}(h) \le \Delta V^{\text{north}}_{\max}(h)\} \end{aligned} \tag{15}$$

If the east and north velocity errors are assumed to be independent, the desired probability will be

$$P_{\text{good}}(h) = P_{\text{east}}(h)P_{\text{north}}(h) \tag{16}$$

In our case, a successful mission is performed if the trajectory intercepts the release zone at an altitude between h_1 and h_2. Therefore, the "success" probability can be defined as the probability that the trajectory errors are not greater than the maximum allowable ones for an altitude between h_1 and h_2, and so if we define $A(h)$ as the event "the release zone is intercepted at altitude h," it follows that

$$\bar{P}_{\text{good}} = \Pr\left\{\bigcup_{h=h_1}^{h_2} A(h)\right\} \Rightarrow \bar{P}_{\text{good}} \ge \Pr\{A(h)\} \Rightarrow \bar{P}_{\text{good}} \ge P_{\text{good}}(h) \qquad h_1 \le h \le h_2 \tag{17}$$

Therefore, we can take the maximum value of $P_{\text{good}}(h)$ in the range $[h_1, h_2]$ still having a conservative estimation of the success probability $\bar{P}_{\text{good}}$, that is,

$$\hat{P}_{\text{good}} = \max_{h\in[h_1,h_2]} P_{\text{good}}(h) \le \bar{P}_{\text{good}} \tag{18}$$

Finally, it is possible to find the optimal free lift f_{opt} by solving the following optimization problem:

$$P_{\text{opt}} = \max_{F_L} \hat{P}_{\text{good}} \tag{19}$$

Therefore, the optimal mass of gas $M^{\text{gas}}_{\text{opt}}$ can be calculated by using Eq. (20):

$$f = (\sigma - 1)\frac{M_{\text{gas}}}{M_{\text{gr}} + M_{\text{bal}}} \tag{20}$$

It is worth noting that the free lift is constrained to stay within a certain range, because two structural limitations exist. The first limitation $F_{L_{\max}}$ (or $f_{\max}$) is related to mechanical resistance of the balloon film. In fact, if the ascent velocity is too high, the film may cool below its glass transition temperature, possibly causing a balloon burst with consequent mission failure. The second $F_{L_{\min}}$ (or $f_{\min}$) is instead related to the total mass that the balloon can carry. It is practically the buoyancy force corresponding to the minimum acceptable rate of ascent. These constraints provide two limits on the acceptable mass of gas:

$$f_{\min} = (\sigma - 1)\frac{M^{\text{gas}}_{\min}}{M_{\text{gr}} + M_{\text{bal}}} \Rightarrow M^{\text{gas}}_{\min} = \frac{f_{\min}(M_{\text{gr}} + M_{\text{bal}})}{(\sigma - 1)} \tag{21}$$

$$f_{\max} = (\sigma - 1)\frac{M^{\text{gas}}_{\max}}{M_{\text{gr}} + M_{\text{bal}}} \Rightarrow M^{\text{gas}}_{\max} = \frac{f_{\max}(M_{\text{gr}} + M_{\text{bal}})}{(\sigma - 1)} \tag{22}$$

Finally, considering that the exact value of gas mass is not known at liftoff, it can be useful to evaluate the allowable uncertainties on the free lift that still guarantee an acceptable success probability. More in detail, it is possible to find the maximum free lift $\bar{F}_{L_{\max}}$ (or $\bar{f}_{\max}$) and minimum free lift $\bar{F}_{L_{\min}}$ (or $\bar{f}_{\min}$) corresponding to a minimum acceptable probability $p_0 < P_{\text{opt}}$ (see Fig. 3):

$$\bar{f}_{\max}|\hat{P}_{\text{good}} = p_0 \qquad \bar{f}_{\min}|\hat{P}_{\text{good}} = p_0 \tag{23}$$

As a consequence, assuming that it is possible to compensate a (negative) gas mass error through ballast discharge during flight, the maximum allowable uncertainties on the gas mass ($\Delta M^{\text{upper}}_g \ge 0$, $\Delta M^{\text{lower}}_g \le 0$) that still guarantee a success probability greater than p_0 are given by Eqs. (24):

$$\begin{aligned} \bar{f}_{\max} &= (\sigma - 1)\frac{M^{\text{opt}}_{\text{gas}} + \Delta M^{\text{upper}}_g}{M_{\text{gr}} + M_{\text{bal}}} \Rightarrow \Delta M^{\text{upper}}_g \\ &= \frac{\bar{f}_{\max}(M_{\text{gr}} + M_{\text{bal}})}{(\sigma - 1)} - M^{\text{opt}}_{\text{gas}} \\ \bar{f}_{\min} &= (\sigma - 1)\frac{M^{\text{opt}}_{\text{gas}} + \Delta M^{\text{lower}}_g}{M_{\text{gr}}} \Rightarrow \Delta M^{\text{lower}}_g = \frac{\bar{f}_{\min} M_{\text{gr}}}{(\sigma - 1)} - M^{\text{opt}}_{\text{gas}} \end{aligned} \tag{24}$$

IV. Procedure for Launch Decision Making

In this section, we will describe an operative procedure to support the decision-making process during the hours preceding the launch. This procedure relies on the statistical analysis carried out in Sec. II and on the optimization algorithms described in Sec. III. The procedure described next has been used during the DTFT1 mission campaign for the selection of the best day to perform the mission and for the definition of the correct balloon parameters. Obviously, this procedure is not concerned with ground wind conditions which, of course, must be monitored to verify the feasibility of the launch operations. The procedure is briefly described next.

For each update of the ECMWF weather forecast, the optimization method described in the previous section is capable of giving the optimum balloon parameters, the predicted trajectory, and the related success probability as defined in Sec. III. If this probability is greater

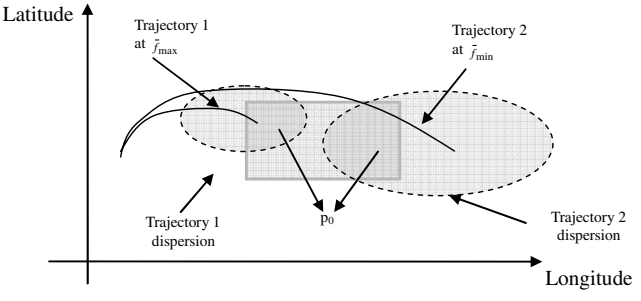

Fig. 3 Maximum and minimum free lift with probability p_0.

Table 2 Decision thresholds

Forecast	Prediction reliability index
−66 h	75.0%
−54 h	80.0%
−42 h	85.0%
−30 h	90.0%
−18 h	95.0%

than a given threshold (see Table 2), launch operations are confirmed until the next forecast update. Conversely, the decision to launch is left to the Mission Board which makes further evaluations, mainly related to safety constraints and mission requirements. If the success probability is zero, launch operations are stopped.

The aforementioned decision thresholds are reported in Table 2, and they are obtained by computing the probability I_1 (see Sec. II) for the forecast-based predictions at different hours. It will be shown that such probability is greater than the average success probability when a generic predicted trajectory is successful. Therefore, we decided to consider the overcoming of the threshold as a sufficient condition to state that the launch conditions are suitable enough to accomplish the mission successfully.

Let us consider two random variables x and y which represent, respectively, the predicted trajectory and the actual trajectory. We can define two events S_x and S_y as follows:

$$\begin{cases} S_x = [x_1 \le x \le x_2] \\ S_y = [y_1 \le y \le y_2] \end{cases} \tag{25}$$

where S_x means that the predicted trajectory is successful and S_y means that the actual trajectory is successful. Therefore, the decision threshold is the probability of the event S_y conditioned to the event S_x. Now, recalling that, from Bayes' theorem [17], the following equality holds

$$\Pr\{S_y|S_x\} = \frac{\Pr\{S_x, S_y\}}{\Pr\{S_x\}} \tag{26}$$

we have

$$\Pr\{S_y|S_x\} = \frac{\int_{x_1}^{x_2}\int_{y_1}^{y_2} f_{x,y}(x,y)\,\mathrm{d}y\,\mathrm{d}x}{\Pr\{S_x\}} = \frac{\int_{x_1}^{x_2}\int_{y_1}^{y_2} f_{y|x}(y|x)\,\mathrm{d}y f_x(x)\,\mathrm{d}x}{\Pr\{S_x\}} \tag{27}$$

where $f_{x,y}(x,y)$ is the joint probability density function of (x,y), and we exploited Bayes' theorem for the density functions, that is,

$$f_{x,y}(x,y) = f_{y,x}(y,x) = f_{y|x}(y|x) f_x(x) \tag{28}$$

The inner integral of Eq. (27) is just the probability of the event S_y conditioned to the value of x, $\Pr\{S_y|x\}$, then we have

$$\Pr\{S_y|S_x\} = \frac{\int_{x_1}^{x_2} \Pr\{S_y|x\} f_x(x)\,\mathrm{d}x}{\Pr\{S_x\}} \tag{29}$$

It is easy to see that the numerator of Eq. (29) is just the mean (computed over the successful predicted trajectories) of S_y conditioned to the trajectory x; then we have

$$\Pr\{S_y|S_x\} = \frac{E_{x_1\le x\le x_2}[\Pr\{S_y|x\}]}{\Pr\{S_x\}} \ge E_{x_1\le x\le x_2}[\Pr\{S_y|x\}] \tag{30}$$

since $\Pr\{S_x\} \le 1$.

V. DTFT1 Postflight Analysis

In this section, the effectiveness of the method used for the ascent trajectory prediction and optimization during the overall DTFT1 test campaign will be assessed. The analysis will be carried out by exploiting the results achieved during the flight campaign that ended on 24 February 2007 with the launch of the FTB 1 vehicle and DTFT1 mission accomplishment. The main objectives of this postflight analysis are the verification of the accuracy of the estimation of the trajectory prediction errors and the verification of the effectiveness of the operative procedure described in Sec. IV. The analysis exploits the following data: 1) statistical analysis carried out before the launch window; 2) daily ECMWF weather forecast data at −66, −54, −42, −30, −18, and −6 h; 3) daily prediction and optimization of the ascent trajectory as described in Secs. II and III; and 4) daily soundings carried out at 07 UTC using typical weather balloons [18] (a total of 33 soundings during the flight campaign).

A. Trajectory Prediction Error

During the flight campaign, several soundings were carried out. The sounding trajectories have been compared with daily predicted trajectories to evaluate the reliability of the trajectory prediction. As an example, Figs. 4 and 5 show a comparison between a sounding and the related trajectory prediction made 18 and 6 h before.

The dashed trajectory is the sounding carried out on 17 January 2007 at 07 UTC and the solid trajectory is the related predicted trajectory. The asterisks mark the points corresponding to the altitude of 20 km (nominal release altitude of DTFT1). We recall that the sounding trajectory is representative of an actual trajectory, whereas the predicted trajectory is a simulated trajectory having the same altitude profile of the sounding balloon and using forecast winds. It is worth noting that, during the flight campaign, the soundings were carried out using weather balloons whose flight

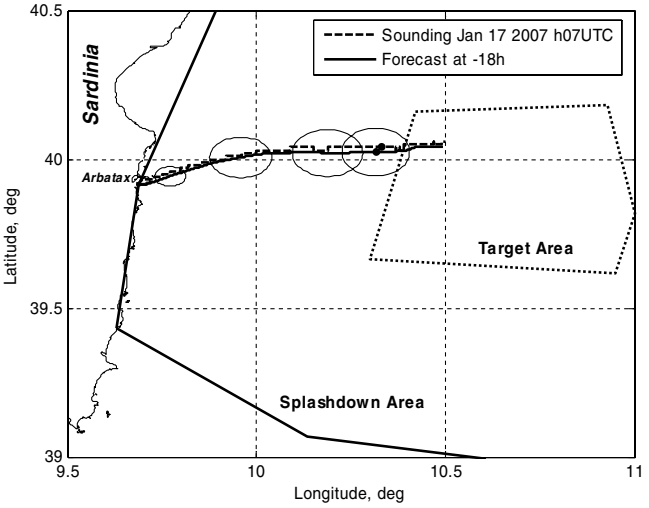

Fig. 4 Sounding at 07 UTC and predicted trajectory at −18 h.

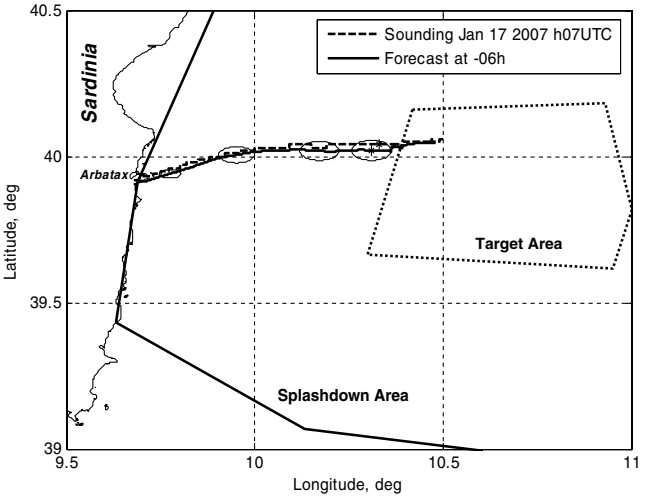

Fig. 5 Sounding at 07 UTC and predicted trajectory at −06 h.

behavior cannot be simulated (using ACHAB) because it is quite different from the one of zero-pressure balloons. Hence, to compare the predicted trajectories with the actual ones (soundings) in terms of horizontal velocity errors, we simply computed the predicted trajectory using the sounding altitude profile (assuming zero error between predicted and actual rate of climb as previously done) and integrating the related horizontal wind velocities. In this way, the reliability of the trajectory prediction was verified using actual (not simulated) trajectories.

As we can see from the figures, there is a very good agreement between actual data and predicted ones. Nevertheless, although almost all predicted trajectories have been in very good agreement with the actual ones, there were some days in which the agreement was poor, that is, the actual trajectory was outside the dispersion ellipse given by the statistical analysis. Further analysis using predicted trajectories and trajectories simulated with ECMWF analysis data at 06 UTC showed that the most likely reason for such poor agreement in the aforementioned cases is that sounding trajectories refer to 07 UTC whereas predicted trajectories refer to 06 UTC. Furthermore, this difference is noticeable only when meteorological conditions are rapidly changing. Anyhow, such meteorological conditions would prevent launch operations, therefore the performed analysis can still be considered valid in all the cases which are suitable for a safe accomplishment of the launch.

Finally, in Fig. 6, the actual DTFT1 balloon trajectory (solid line) and its forecast at −18 h (dotted line) are depicted; the star represents the actual release point (at about 20 km of altitude), whereas the triangle represents the predicted release point. The predicted trajectory was obtained using ACHAB with wind forecast and the actual gas mass transferred to the balloon at inflation. As we can see from Fig. 6, the dispersion zone allowed us to reliably identify the actual release point. It is worth emphasizing that, although the success probability computed through the optimization process was less than the decision threshold (see Sec. IV), the launch was confirmed by the Mission Board. As a matter of fact, balloon trajectory prediction allowed a safe splashdown of all of the system parts (vehicle, gondola, balloon), provided that the actual release point was sufficiently to the east (even if outside the release zone). Therefore, the Mission Board decided to operate the launch nominally.

B. Effectiveness of the Operative Procedure

Concerning the effectiveness of the operative procedure used as a support for the decision-making process during the entire test campaign, we observed that when the procedure issued a "positive to launch" decision, the sounding at launch hour was successful, and when the procedure issued a "negative to launch" decision, the sounding at launch hour was unsuccessful. The results are summarized in Table 3. Therefore, we can conclude that the analysis of experimental data demonstrated the effectiveness of the proposed method.

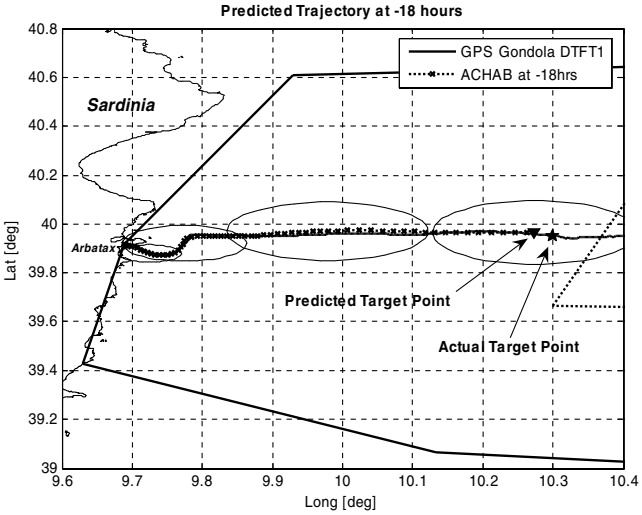

Fig. 6 February 24 2007: actual balloon trajectory and forecast at −18 h.

Table 3 Operative procedure results

	Procedure outcomes	Launch hour sounding outcomes
Negative to launch	13	13
Positive to launch	5	5
Decision left to board	15	——

VI. Conclusions

In this paper, a method for the prediction and optimization of the ascent trajectory of a stratospheric balloon to target a specified 3-D flight area has been proposed.

The described method mainly relies on the following points: 1) an accurate statistical estimation of the trajectory prediction errors and its direct application to nominal trajectory simulation without using Monte Carlo analysis; 2) an algorithm that maximizes the probability of reaching a predefined target area taking into account wind forecast uncertainties; and 3) the use of a procedure based on the statistical theory to select the right day to perform the mission.

The proposed methodology has been successfully used during the DTFT1 mission accomplished by Italian Aerospace Research Center. Its effectiveness has been verified by means of a postflight analysis carried out with the experimental data collected throughout the test campaign.

References

[1] Palumbo, R., Russo, M., Filippone, E., and Corraro, F., "ACHAB: Analysis Code for High-Altitude Balloons," *AIAA Atmospheric Flight Mechanics Conference and Exhibit*, AIAA Paper 2007-6642, 2007.

[2] Morris, A. (ed.), "Scientific Ballooning Handbook," National Center for Atmospheric Research, TN/1A-99, 1975.

[3] Pankine, A. A., Heun, M. K., Nguyen, N., and Schlaifer, R. S., "NAVAJO: Advanced Software Tool for Balloon Performance Simulation," *AIAA 5th Aviation Technology, Integration and Operations Conference (ATIO)*, AIAA Paper 2005-7411, 2005.

[4] Pankine, A. A., Heun, M. K., and Schlaifer, R. S., "Advanced Balloon Performance Simulation and Analysis Tool," *AIAA 3rd Annual Aviation Technology, Integration and Operations (ATIO)*, AIAA Paper 2003-6741, 2003.

[5] Kreith, F., and Kreider, J. F., "Numerical Prediction of the Performance of High-Altitude Balloons," National Center for Atmospheric Research Technical Notes, NCAR TN/STR-65, Feb. 1974.

[6] Carlson, L. A., and Horn, W. J., "New Thermal and Trajectory Model for High-Altitude Balloons," *Journal of Aircraft*, Vol. 20, No. 6, 1983, pp. 500–507. doi:10.2514/3.44900

[7] De Giorgis, M., Borriello, G., Allasio, A., Vavala, R., Leveugle, T., and Cosentino, O., "Atmospheric Reentry Demonstrator Balloon Flight Test," *Journal of Spacecraft and Rockets*, Vol. 36, No. 4, July–Aug. 1999, pp. 507–510.

[8] Russo, G., Carmicino, C., de Matteis, P., Marini, M., Rufolo, G., Di Palma, L., Belardo, M., Corraro, F., and Verde, L., "Unmanned Space Vehicle Program: DTFT in Flight Experiments," *18th ESA Symposium on European Rocket and Balloon Programmes and Related Research*, ESA Communication Production Office, European Space Research and Technology Center, Noordwijk, The Netherlands, Nov. 2007, pp. 89–96.

[9] Musso, I., Cardillo, A., and Cosentino, O., "Software and Methodologies for Stratospheric Balloons' Flight Prediction," *3rd AIAA Aviation Technology, Integration and Operations Technical Forum*, AIAA Paper 2003-6820, 2003.

[10] Cardillo, A., Musso, I., Ibba, R., and Cosentino, O., "USV Test Flight by Stratospheric Balloon: Preliminary Mission Analysis," *Advances in Space Research*, Vol 37, No. 11, 2006, pp. 2038-2042. doi:10.1016/j.asr.2005.04.067.

[11] Musso, I., Cardillo, A., Cosentino, O., and Memmo, A., "A Balloon Trajectory Prediction System," *Advances in Space Research*, Vol. 33, No. 10, 2004, pp. 1722–1726. doi:10.1016/j.asr.2003.07.044

[12] Musso, I., Cardillo, A., and Ibba, R., "Genetic Algorithm: Trajectory Optimization for Stratospheric Balloons," *17th ESA Rockets and Balloons Research Symposium*, ESA SP-590, ESA Publ. Div., Noordwijk, The Netherlands, 2005, 457–460.

[13] Musso, I., Cardillo, A., and Cosentino, O., "The HASI Flight Control Strategy," *23rd International Symposium on Space Technology and Science* Paper ISTS 2002-m-02, 2002.

[14] Musso, I., Cardillo, A., Ibba, R., Spoto, D., Peterzen, S., Masi, S., and Memmo, A., "Enhancement on Stratospheric Balloons Trajectory Prediction, Optimization and Monitoring," *18th ESA Symposium on European Rocket and Balloon Programmes and Related Research*, ESA Communication Production Office, European Space Research and Technology Center, Noordwijk, The Netherlands, Nov. 2007, pp. 331–336.

[15] Lai, C., Cuciniello, G., Nebula, F., Palumbo, R., Russo, M., Vitale, A., and Corraro, F., "A Stratospheric Balloon Integrated Navigation Facility," *18th ESA Symposium on European Rocket and Balloon Programmes and Related Research*, ESA Communication Production Office, European Space Research and Technology Center, Noordwijk, The Netherlands, Nov. 2007, pp. 341–346.

[16] Chernoff, H., "A Measure of Asymptotic Efficiency for Test of Hypothesis on the Sum of Observations," *Annals of Mathematical Statistics*, Vol. 23, No. 4, 1952, pp. 493–507. doi:10.1214/aoms/1177729330

[17] Papoulis, A., *Probability, Random Variables, and Stochastic Processes*, 3rd ed., McGraw–Hill, New York, 1991, Chaps. 4, 6.

[18] Palumbo, R., Mercogliano, P., Corraro, F., De Matteis, P. P., and Sabatano, R., "Meteorological Conditions Forecast and Balloon Trajectory Estimations," *Memorie della Società Astronomica Italiana* (to be published).

J. Martin
Associate Editor